

Journal Pre-proof

Neohesperidin inhibits TGF- β 1/Smad3 signaling and alleviates bleomycin-induced pulmonary fibrosis in mice

Jiasen Guo, Yinshan Fang, Fangxin Jiang, Lian Li, Honggang Zhou, Xiaojun Xu, Wen Ning



PII: S0014-2999(19)30664-8

DOI: <https://doi.org/10.1016/j.ejphar.2019.172712>

Reference: EJP 172712

To appear in: *European Journal of Pharmacology*

Received Date: 1 April 2019

Revised Date: 26 September 2019

Accepted Date: 30 September 2019

Please cite this article as: Guo, J., Fang, Y., Jiang, F., Li, L., Zhou, H., Xu, X., Ning, W., Neohesperidin inhibits TGF- β 1/Smad3 signaling and alleviates bleomycin-induced pulmonary fibrosis in mice, *European Journal of Pharmacology* (2019), doi: <https://doi.org/10.1016/j.ejphar.2019.172712>.

This is a PDF file of an article that has undergone enhancements after acceptance, such as the addition of a cover page and metadata, and formatting for readability, but it is not yet the definitive version of record. This version will undergo additional copyediting, typesetting and review before it is published in its final form, but we are providing this version to give early visibility of the article. Please note that, during the production process, errors may be discovered which could affect the content, and all legal disclaimers that apply to the journal pertain.

© 2019 Published by Elsevier B.V.

Neohesperidin inhibits TGF- β 1/Smad3 signaling and alleviates bleomycin-induced pulmonary fibrosis in mice

Jiasen Guo^{a,*}, Yinshan Fang^{a,*}, Fangxin Jiang^a, Lian Li^{a,b}, Honggang Zhou^c, Xiaojun Xu^{d,#},
Wen Ning^{a,#}

^aState Key Laboratory of Medicinal Chemical Biology, College of Life Sciences, Nankai University, Tianjin 300071, China

^bRespiratory Department, Tianjin Medical University General Hospital, Tianjin 300071, China

^cState Key Laboratory of Medicinal Chemical Biology, College of Pharmacy, Nankai University, Tianjin 300071, China

^dState Key Laboratory of Natural Medicines, China Pharmaceutical University, Nanjing 211198, China

* Indicates equal first authorship.

Indicates equal senior authorship.

[#]Correspondence to: Nankai University, 94 Weijin Road, Tianjin 300071, China.

E-mail addresses: ningwen108@nankai.edu.cn (W. Ning), xiaojunxu2000@163.com (X. Xu).

ABSTRACT

Idiopathic pulmonary fibrosis (IPF) is a fatal growing problem, with limited therapeutic options. Transforming growth factor beta 1 (TGF- β 1) plays a critical role in many pathological processes that characterize pulmonary fibrosis. Effective and well-tolerated antifibrotic agents that interfere with TGF- β 1 signaling would be an ideal treatment but no such treatments are available. In this study, we identified that the natural compound, neohesperidin, antagonizes TGF- β 1/Smad3 signaling. We found that neohesperidin not only inhibited the TGF- β 1-induced injury to alveolar epithelial cells but also decreased the TGF- β 1-induced myofibroblast differentiation, extracellular matrix production, and fibroblast migration. Furthermore, we obtained *in vivo* evidence that neohesperidin treatment inhibited bleomycin-induced lung injuries and even attenuated established pulmonary fibrosis in mice. Our data suggest that neohesperidin can target the critical signaling pathway and profibrogenic responses in progressive pulmonary fibrosis and may have a potential use in treatment.

Keywords: Neohesperidin, Pulmonary fibrosis, TGF- β 1, Fibroblast

1. Introduction

Idiopathic pulmonary fibrosis (IPF) is a chronic, progressive, devastating, and fatal interstitial lung disease, characterized by patchy subpleural parenchymal fibrosis, with pathological features including the accumulation of myofibroblasts, formation of fibroblast foci, distortion of the pulmonary architecture, and increased collagen deposition (Raghu et al., 2004). The incidence of IPF is estimated to be 14.0–42.7 per 100,000 people in the U.S. (Raghu et al., 2006), and the mean survival of IPF patients from the time of diagnosis is only 2.5–3.5 years (King et al., 2011). In 2014, two drugs, pirfenidone and nintedanib, were approved for the treatment of IPF (Mora et al., 2017). However, IPF remains an incurable disease, which makes it vital for innovative studies to develop new treatment strategies.

IPF is an epithelial-fibroblastic disorder that results from numerous micro injuries to the alveolar epithelia and subsequent induction of excessive fibroblast activity. After an injury to the lung's epithelia, important profibrotic mediators such as transforming growth factor TGF- β 1 are released by epithelial cells, fibroblasts, and other cell types (Selman and Pardo, 2012). There are evidence that TGF- β 1 is critical for the progression of pulmonary fibrosis in mice due to its role in regulating epithelial cell apoptosis, fibroblast proliferation, myofibroblast differentiation, and collagen synthesis. TGF- β 1 is upregulated in lung tissues of both bleomycin-injured mice (Hoyt and Lazo, 1988) and IPF patients (Khalil et al., 1991). Overexpression of active TGF- β 1 induces prolonged and severe interstitial lung fibrosis in rats (Sime et al., 1997). Deletion of TGF- β receptor II from either fibroblast (Hoyle et al., 2011) or epithelial cells (Li et al., 2011) protects mice from bleomycin-induced pulmonary fibrosis. Although the profibrotic role of TGF- β 1 signaling has been well studied, only few

candidates that directly target the TGF- β 1 signaling pathway have reached early phase clinical trials because of their toxicity.

Natural compounds have been investigated by researchers as a source of substitutes for fibrosis remedies because of their low toxicity and costs. Neohesperidin, composed of the flavanone hesperetin and disaccharide neohesperidoside (Fig. 1A), is a natural flavonoid unique to specific citrus cultivars and shows no apparent toxicity. Its biological activities, such as neuroprotective activity (Hwang and Yen, 2008), radical scavenging (Lee et al., 2009), antiproliferative effects (Bellocco et al., 2009), proapoptotic effects (Xu et al., 2012), and hypoglycemic activity (Jia et al., 2015), have been intensively studied, but this natural molecule is likely to have a much broader therapeutic potential than what is currently known to have. Here, we investigated effects of neohesperidin on the TGF- β 1 signaling, TGF- β 1-induced lung fibroblast activation and epithelial injury *in vitro*. We further examined the potential role of neohesperidin in pulmonary fibrosis and inflammatory response in the bleomycin-injured mice *in vivo*.

2. Materials and methods

2.1. Chemicals

Neohesperidin with over 99% purity was purchased from Selleckchem (TX, USA), and bleomycin was purchased from Nippon Kayaku (Tokyo, Japan). The other chemicals used were of analytical grade.

2.2. Cell lines and mice

The mouse embryonic fibroblast NIH-3T3, mouse lung fibroblast MLg, and human alveolar epithelial cell (AEC) A549 lines were obtained from American Type Culture Collection (ATCC). NIH-3T3 cells were transfected with the CAGA-luciferase reporter gene to generate CAGA-NIH-3T3 reporter cells. Cells were routinely cultured in Dulbecco's modified Eagle's medium (DMEM) supplemented with 10% fetal bovine serum (FBS) and antibiotics (100 U/ml penicillin and 100 µg/ml streptomycin) in an incubator with 5% CO₂ at 37 °C.

Eight-week old male C57BL/6J mice were purchased from Vital River Laboratories (Beijing, China). All mice were housed in a pathogen-free facility at Nankai University. The animal experimental protocol was approved by the Animal Care and Use Committee at Nankai University. All operations were performed under 7.5% chloral hydrate anesthesia, and all efforts were made to minimize animal suffering.

2.3. Bleomycin administration and experimental design

Mouse pulmonary fibrosis was established as previously described (Dong et al., 2015). Briefly, mice were intratracheally injected with a single dose of bleomycin (2.5 or 5 U/kg body weight) dissolved in physiological saline (0.9% NaCl) and then randomly divided into two groups, a control group and neohesperidin treated group. The mice in the latter group were i.p. injected with 20 mg/kg neohesperidin, which was suspended in a 0.5% sodium carboxymethyl cellulose (CMC-Na) solution, while the mice in the control group were injected with an equal volume of saline. At the indicated times after bleomycin treatment, the

mice were killed for subsequent experiments.

2.4. Luciferase assay

CAGA-NIH-3T3 cells were seeded in a 96-well plate and after reaching 80% confluence, were serum starved for 24 h. Thereafter, the cells were treated with different concentrations of neohesperidin for 1 h and with 5 ng/ml TGF- β 1 for 24 h in DMEM containing 0.1% FBS. At the end of the treatment, cells were lysed and assayed in a dual-luciferase reporter assay (Promega) according to the manufacturer's instructions. The total light emission during the initial 20 s of the reaction was measured in a luminometer (Lumat LB 9501; Berthold).

2.5. Cell viability analysis

MLg cells were seeded in a 96-well plate and pre-treated with different concentrations of neohesperidin for 1 h and then co-cultured with or without TGF- β 1 (10 ng/ml) as indicated. Cell viability was determined using 3-(4,5-dimethylthiazol-2-yl)-2,5-diphenyltetrazolium bromide (MTT) Cell Proliferation and Cytotoxicity Assay Kit (Beyotime, China) according to the manufacturer's instructions.

2.6. RNA extraction and quantitative real-time polymerase chain reaction

RNA isolation and quantitative real-time polymerase chain reaction (qRT-PCR) were performed as previously described (Fang et al., 2017). Total RNA was extracted from cells using the TRIzol reagent according to the manufacturer's instruction. First-strand

complementary DNA (cDNA) was synthesized using random oligonucleotide primers and M-MLV reverse transcriptase. qRT-PCR was carried in a 20 µl volume containing 5 pmol primers, 10 ng of cDNA, and a SYBR Green PCR master mix. Gene expression was determined relative to that of the endogenous reference gene (β -actin) using the $2^{-\Delta\Delta Ct}$ method. The target genes and their primer sequences were as follows: *Acta2* [encoding alpha-smooth muscle actin (α -SMA)], 5'-GCTGGTGATGATGCTCCCA-3' and 5'-GCCCATTCOAACCATTACTCC-3'; *Coll1a1* [encoding type I collagen (COL1)], 5'-CCAAGAAGACATCCCTGAAGTCA-3' and 5'-TGCACGTCATCGCACACA-3'; *Fnl1* (encoding fibronectin 1), 5'-GTGTAGCACAACCTTCCAATTACGAA-3' and 5'-GGAATTTCCGCCTCGAGTCT-3'; *Actb* (encoding β -actin), 5'-AGGCCAACCGTGAAAAGATG-3' and 5'-AGAGCATAGCCCTCGTAGATGG-3'; *CDH1* (encoding E-cadherin), 5'-CGAGAGCTACACGTTACACGG-3' and 5'-TGCACGTCATCGCACACA-3'; *CDH2* (encoding N-cadherin), 5'-TCAGGCGTCTGTAGAGGCTT-3' and 5'-ATGCACATCCTTCGATAAGACTG-3'; and *SNAIL* (encoding SNAIL), 5'-TCGGAAGCCTAACTACAGCGA-3' and 5'-AGATGAGCATTGGCAGCGAG-3'; *ACTB* (encoding β -actin), 5'-CATGTACGTTGCTATCCAGGC-3' and 5'-CTCCTTAATGTCACGCACGAT-3'.

2.7. Western blotting

Western blot analysis was performed following standard protocol, as previously described (Ning et al., 2004). Proteins were extracted from both cells and culture supernatants. Culture media were collected and centrifuged at $14,000 \times g$ for 3 min at 4 °C to remove dead cells.

The total protein was obtained from the medium using a traditional trichloroacetic acid (TCA)–acetone precipitation method. Briefly, one part of TCA was mixed with nine parts of a supernatant, and the mixture was incubated for 30 min on ice, followed by centrifugation at $14,000 \times g$ for 30 min at $4\text{ }^{\circ}\text{C}$. The precipitate was washed and precipitated with acetone. After being dried at room temperature for approximately 10 min, the protein sample was dissolved in a loading buffer. Cells were homogenized in radioimmunoprecipitation assay buffer containing phenylmethylsulfonyl fluoride, and the homogenates were centrifuged at $14,000 \times g$ for 15 min at $4\text{ }^{\circ}\text{C}$. The supernatants were collected, and the protein concentrations were determined using the bicinchoninic acid assay. Equal amounts of proteins were separated by sodium dodecyl sulfate polyacrylamide gel electrophoresis and blotted onto polyvinylidene difluoride membranes. The membranes were blocked with 5% nonfat milk at room temperature for 1 h and incubated at $4\text{ }^{\circ}\text{C}$ overnight with primary antibodies. Antibodies to phosphorylated (p)-Smad2 (3108), Smad2 (3122), p-Smad3 (9520), Smad3 (9513), p-extracellular signal-regulated kinase (ERK; 4370S), ERK (4695), p-p38 (4631S), p38 (9212), p-c-Jun N-terminal kinase (JNK; 9251S), JNK (9252), E-cadherin (3195), N-cadherin (13116), and SNAIL (3879) were purchased from Cell Signaling Technology. Antibodies to type I collagen (ab21286) and fibronectin (ab2413) were purchased from Abcam. Antibodies to glyceraldehyde 3-phosphate dehydrogenase (GAPDH; UM4002) and β -tubulin (UM4003) were purchased from Utibody Biotechnology. An antibody to α -SMA (sc-32251) was purchased from Santa Cruz Biotechnology, and that to β -actin (AC026) was purchased from ABclonal Technology. Subsequently, the membranes were incubated with horseradish peroxidase (HRP)-conjugated secondary antibodies at room

temperature for 2 h, and protein signals were detected using an enhanced chemiluminescence kit (Pierce).

2.8. Cell migration assay

Migration was assessed by a wound healing assay. MLg cells were seeded in a six-well plate and cultured for 24 h. After scraping the cell monolayer with a sterile micropipette tip, the cells were treated with neohesperidin (20 μ M) in the presence and absence of TGF- β 1 (10 ng/ml) for 36 h. The scratch was captured using bright field microscopy (Olympus, Japan). Images were obtained for analysis using Image J software.

2.9. Evaluation of pulmonary function

Mice were anesthetized, tracheostomized, paralyzed, and mechanically ventilated with a computer-controlled small animal ventilator to determine the pulmonary function using an Anires2005 system (Beijing Biolab, China). This system can automatically calculate and display pulmonary parameters such as respiratory dynamic compliance (C_{dyn}), resistance of the lung (RL), and resistance of expiration (RE).

2.10. Histological examination

The left lungs were inflated with 0.4 ml of 10% formalin in phosphate-buffered saline (PBS). Tissues were fixed overnight, embedded in paraffin, and sectioned for staining with hematoxylin and eosin (H&E) or Masson's trichrome. The ImagePro Plus version 6.0

software (Media Cybernetics) was used to analyze digital images. The overall and fibrotic areas of the lung were outlined, and the fibrotic pixels versus total pixels were summed for each lung to obtain the percentage of fibrosis.

2.11. Hydroxyproline assay

Collagen contents were measured in the right lungs, cleared of blood, using a conventional hydroxyproline method (Jiang et al., 2004). The lungs were dried for 16 h at 120 °C, and lung tissues, minced in 3 ml of 6 N HCl, were incubated for another 16 h at 120 °C. The samples were then cooled down and filtered through a 5.0- μ m syringe filter, followed by adjustment of pH to 6.5–8.0 with NaOH. Subsequently, PBS was added to a total volume of 10 ml, and a hydroxyproline assay was performed with chloramine-T by measuring absorbance spectrophotometrically. The completeness of collagen hydrolysis and recovery of hydroxyproline was determined using a sample containing a known amount of purified collagen.

2.12. Bronchoalveolar lavage fluid collection and cell counting

Bronchoalveolar lavage fluid (BALF) was collected as previously described (Dong et al., 2015). Briefly, the trachea was cannulated and lavaged three times with 0.8 ml of sterile PBS at room temperature. Samples were centrifuged at $300 \times g$ for 5 min, and the cell-free supernatants were collected. The pellets were washed with PBS and then suspended in 200 μ l of PBS for total cell counting with a hemocytometer and differential cell counting. For

differential cell counts, smears of each suspension were stained with H&E, and 500 cells were categorized as macrophages, neutrophils, or lymphocytes, based on standard morphological criteria.

2.13. Enzyme-linked immunosorbent assay

Levels of interleukin (IL)-1 β , interferon (IFN)- γ , and tumor necrosis factor (TNF)- α in BALF were measured using commercial enzyme-linked immunosorbent assay (ELISA) kits (BioLegend, USA) according to the manufacturer's instructions. Briefly, BALF samples were added to wells of an assay plate coated with a capture antibody. After overnight incubation, the assay plate was washed three times, and a detection antibody was added. After 1-h incubation at room temperature and washing the plate three times, streptavidin–HRP was added to the wells. The color was developed with the tetramethylbenzidine substrate, and the absorbance was measured at 450 and 570 nm.

2.14. Statistical analysis

Data were processed using the Prism version 7.0 software and expressed as the mean \pm standard error of the mean (SEM). Normal distribution of data was determined using Shapiro-Wilk normality test with Welch's correction if variances differed. For parametric data, significance was analyzed using an unpaired Student's t-test. Non-parametric data were analyzed using Mann–Whitney test. When more than two groups were being compared, one-way or two-way analysis of variance (ANOVA) followed by Tukey's post-hoc test for parametric data was used; the non-parametric data were analyzed by Kruskal–Wallis followed

by Dunn's test. Survival curves were compared using a log-rank test. A two-sided *P*-value of < 0.05 was considered statistically significant.

3. Results

3.1. Neohesperidin suppresses TGF- β 1-activated Smad3 signaling

We evaluated the effect of neohesperidin on TGF- β 1 signaling pathway in NIH-3T3 cells transfected with the (CAGA)₁₂-luciferase reporter, which contained 12 copies of the Smad-binding site. The results showed that this reporter was activated upon TGF- β 1 treatment but was inhibited by neohesperidin in a concentration-dependent manner (Fig. 1B). Our data suggested a new potential role for neohesperidin as an antifibrotic agent via antagonizing TGF- β 1 signaling pathway.

To further explore the intracellular signal transduction mechanism, we examined the effect of neohesperidin on the canonical Smad2/3-dependent pathway and on non-Smad signaling, such as the MAPK cascade, in the mouse lung fibroblast MLg cell line. As shown in Fig. 1C, TGF- β 1 potently increased the levels of phosphorylated Smad2, Smad3, ERK1/2, JNK, and p38, as determined by western blotting. Intriguingly, neohesperidin significantly inhibited the TGF- β 1-induced phosphorylation of Smad3 while showing less effect on TGF- β 1-induced phosphorylation of the other downstream factors (Fig. 1C). These data suggest that neohesperidin blocked TGF- β 1 signaling mainly via the inhibition of the canonical TGF- β 1/Smad2/3 pathway, particularly via inhibition of Smad3 activation.

3.2. Neohesperidin attenuates TGF- β 1-induced lung myofibroblast activation

Fibroblasts and myfibroblasts are the main effector cells, which are activated after tissue injury and in IPF patients, resulting in the elevated production of ECM and enhanced migration potential (Noble et al., 2012; Suganuma et al., 1995). To examine whether neohesperidin mediated a blockade of TGF- β 1 signaling, involved in myfibroblast activation, we used an established *in vitro* model of TGF- β 1-treated fibroblasts. The concentration range of neohesperidin was 5–20 μ M because the compound showed more effect on the viability of MLg cells at concentrations > 25 μ M (Fig. 2A). As shown in Fig. 2B and E, the mRNA and protein expression of α -SMA (a marker of myfibroblast differentiation) significantly increased after TGF- β 1 treatment but was remarkably reduced by neohesperidin intervention, indicating that neohesperidin inhibited the TGF- β 1-induced myfibroblast differentiation. Consistently, TGF- β 1 increased the mRNA and protein levels of two main ECM components, type I collagen and fibronectin, which were markedly decreased when treated with neohesperidin (Fig. 2C–E). In addition, Fig. 2F and G showed that the migration rate of TGF- β 1-stimulated fibroblasts was reduced after 36 h of neohesperidin treatment, suggesting the inhibition of fibroblast migration by neohesperidin. The data revealed the inhibitory effect of neohesperidin on TGF- β 1-induced myfibroblast activation, as indicated by lower levels of myfibroblast differentiation, ECM production, and fibroblast migration.

3.3. Neohesperidin attenuates TGF- β 1-induced lung epithelial injury

An emerging body of literature suggests that AEC injury may be an important early feature in the pathogenesis of pulmonary fibrosis. Injured AECs are activated and likely undergo many

cellular and molecular changes, such as losing epithelial markers and gaining mesenchymal markers at the same time (Wolters et al., 2014). To determine whether blocking of TGF- β 1 signaling by neohesperidin leads to the protection against epithelial injury, we added neohesperidin to TGF- β 1-treated A549 cells. We found that TGF- β 1 induced the epithelial activation, as indicated by a decreased expression of an epithelial marker (E-cadherin) and an increased expression of a mesenchymal marker (N-cadherin), as well as by an increase in the TGF- β 1 downstream transcription factor SNAIL (Fig. 3A and B), which supported the notion that TGF- β 1-injured AECs are activated and may express mesenchymal markers. As expected, neohesperidin intervention significantly inhibited the TGF- β 1-induced epithelial injury in a concentration- and time-dependent manner (Fig. 3A and B). Consistently, qRT-PCR analysis further demonstrated that TGF- β 1 significantly downregulated the mRNA expression of E-cadherin and upregulated that of N-cadherin and SNAIL in A549 cells (Fig. 3C–E). These data suggest that neohesperidin protected alveolar epithelial A549 cells from TGF- β 1-induced injury.

3.4. Neohesperidin alleviates bleomycin-induced pulmonary fibrosis in mice

The antifibrotic effect of neohesperidin was further assessed *in vivo*. We administered bleomycin intratracheally to induce pulmonary fibrosis in mice and found that the mice treated with i.p. injection of neohesperidin (Fig. 4A) were significantly less susceptible to high-dose bleomycin (5 U/kg)-induced lung injury and showed better survival than did the CMC-Na-treated mice (Fig. 4B). Moreover, the neohesperidin-treated mice exhibited an improvement in lung function, as indicated by increased Cdyn and decreased RL/RE values

(Fig. 4C–E). Importantly, neohesperidin treatment attenuated the lung fibrosis. Compared with the mice treated with bleomycin (2.5 U/kg) only, those treated first with bleomycin and 7 days later with neohesperidin (Fig. 5A) showed partial recovery from the fibrosis-induced body weight loss (Fig. 5B) and reduced collagen accumulation, as determined by the hydroxyproline content (Fig. 5C) and Masson's trichrome staining (Fig. 5D). Quantification of the areas of fibrotic lung sections by a blinded pathologist illustrated fibrosis attenuation after neohesperidin treatment (Fig. 5E). The attenuation of fibrosis in the neohesperidin-treated mice was further supported by decreased protein levels for Col1 and α -SMA (Fig. 5F). We also examined the effects of neohesperidin on phosphorylation levels of Smad2/3 *in vivo*. Neohesperidin treatment resulted in a significant decrease in bleomycin-induced phosphorylation of Smad3 (Fig. 5G), confirming that the compound might ameliorate fibrosis by inhibiting TGF- β 1 signaling pathway.

To evaluate whether neohesperidin could reverse an already established fibrosis, we injected neohesperidin 14 days after bleomycin administration, when lung fibrosis was already obvious (Fig. 6A). The mice were killed on day 21, and samples were collected for fibrosis analysis. Notably, neohesperidin significantly reduced the lung fibrosis even after fibrotic disease had been established (Fig. 6B–E). Collectively, these data confirmed neohesperidin as a TGF- β 1 antagonist with a potent antifibrotic activity.

3.5. Neohesperidin is ineffective against bleomycin-induced lung inflammatory response

The bleomycin model is characterized by an initial influx of inflammatory cells (Moeller et al., 2008). To test if neohesperidin treatment could alter this initial inflammatory response

and subsequent fibrosis after bleomycin injury, C57BL/6J mice were first i.p. injected with neohesperidin, followed by bleomycin injury to induce lung fibrosis (Fig. 7A). Surprisingly, the numbers of total and differential inflammatory cells in BALF were comparable in neohesperidin-pretreated mice and in those treated with bleomycin only (Fig. 7B and C). We also measured the cytokines IL-1 β , IFN- γ , and TNF- α , whose dysregulation has been reported in lung tissues of IPF patients and in animal models (Agostini and Gurrieri, 2006; Wynn, 2011). As shown in Fig. 7D–F, the concentrations of these cytokines were similar in BALF from the control and neohesperidin-treated mice. Notably, neohesperidin pretreatment showed less protective effect than its therapeutic effect on lung fibrosis (Fig. 8A–D). Taken together, our data indicated that neohesperidin attenuated the lung fibrosis without affecting the inflammatory response to lung injury in this bleomycin-induced mouse model.

4. Discussion

IPF is a complex, epithelial-driven fibrotic lung disorder. The disease is progressive and lethal, usually within a few years of diagnosis, with limited therapeutic options. Studies have shown several pathogenic pathways and potential therapeutic targets to be explored. Among these, the TGF- β signaling pathway is essential for all profibrotic processes, including epithelial injury, fibroblast activation, and eventual ECM production. Here, we identified a novel activity of a natural small molecule, neohesperidin, which was found to antagonize TGF- β signaling pathway through inhibition of the canonical Smad-dependent pathway. These *in vitro* findings were confirmed in an *in vivo* mouse model, wherein treatment with neohesperidin was proven to effectively attenuate pulmonary fibrosis. The data generated

from the cellular and animal models are encouraging and support the potential therapeutic benefits of neohesperidin for the treatment of patients with progressive pulmonary diseases. A very recent study using cell-based high-content screening also identified neohesperidin has prospective inhibitory activity in TGF- β 1-induced NRK49F rat kidney fibroblast differentiation (Wang et al., 2018), which agrees with our findings that neohesperidin may have anti-fibrotic effect.

Several lines of evidence demonstrated the antifibrotic effects of neohesperidin on progressive pulmonary fibrosis. Neohesperidin antagonized TGF- β 1 signaling, as indicated by decreased Smad3 phosphorylation. Neohesperidin treatment inhibited the TGF- β 1-induced epithelial injury, myofibroblast activation, ECM production, and fibroblast migration *in vitro*, as well as bleomycin-induced pulmonary fibrosis, even established one, *in vivo*. Importantly, the use of neohesperidin offers a clear advantage of safety since neohesperidin is a natural flavonoid, unique to citrus cultivars. Natural compounds are currently considered valuable resources for drug screening and development, and strategies aimed at interfering with TGF- β 1 signaling pathway have been developed to treat IPF. It has recently been reported that baicalin (Huang et al., 2016) and emodin (Guan et al., 2016) can attenuate the bleomycin-induced pulmonary fibrosis, while salvianolic acid B (Liu et al., 2016) is able to protect against paraquat-induced pulmonary injury, with their mechanisms of action all related to the inactivation of TGF- β 1 signaling. Similarly, we showed that neohesperidin antagonized TGF- β 1 signaling, specifically, via its canonical Smad-dependent pathway. It is widely recognized that TGF- β 1 acts by stimulating its downstream mediators Smad2/3 to exert its biological activities in organ fibrosis, including lung fibrosis (Hu et al., 2018).

Although Smad2 and Smad3 physically interact and are structurally similar, with 90% homology in their amino acid sequences (Yagi et al., 1999), distinct roles have been reported for these two Smads in ECM production and tissue fibrosis (Meng et al., 2010). Duncan et al. reported that TGF- β 1 induces the expression of connective tissue growth factor (CTGF) via a functional Smad3-binding site in the *CTGF* promoter, which in turn stimulates the myofibroblast differentiation and collagen synthesis (Duncan et al., 1999). We showed in our *in vitro* and *in vivo* models that Smad3, rather than Smad2, is a potential intracellular transducer targeted by neohesperidin. This finding agrees with the data of recent studies in which Smad3 was recognized as a key mediator of TGF- β 1 signaling in ECM production and tissue fibrosis (Hu et al., 2018; Kang et al., 2017).

IPF is an epithelial-fibroblastic disorder that results from numerous microinjuries to the alveolar epithelium, leading to the induction of excessive fibroblast activity. Activated fibroblasts, i.e., myofibroblasts, are a major source of ECM, which accumulates during fibrosis (Hinz et al., 2012). We found that neohesperidin attenuated the lung fibrosis through its effects on AEC injury and on fibroblasts differentiation and activation. Our data showed that neohesperidin inhibited the function of fibroblasts by significantly reversing the TGF- β 1-induced myofibroblast differentiation, ECM production, and fibroblast migration *in vitro*. These effects may underlie the ability of neohesperidin to counteract the fibrogenic effects of bleomycin *in vivo* and reduce even established bleomycin-induced fibrosis. Meanwhile, when applied prophylactically, neohesperidin treatment did not show a protective effect against bleomycin-induced lung fibrosis in mice.

It has been argued that IPF is a non-inflammatory condition because pulmonary fibrosis fails

to respond to corticosteroid therapy (Byrne et al., 2016). Recently, a more nuanced view of the immune cell function has led to reevaluation of the role of inflammatory cells in the development of pulmonary fibrosis. Interestingly, neohesperidin treatment did not seem to affect the initial influx of inflammatory cells and production of cytokines in the bleomycin model. Importantly, our findings suggest that neohesperidin treatment may attenuate fibrosis at doses that do not exacerbate inflammation, thus avoiding potential risks associated with global TGF- β 1 inhibition.

Although our results demonstrated the potential therapeutic effect of neohesperidin against bleomycin-induced pulmonary fibrosis in mice, its more detailed mechanism of action remains unclear. For example, how does neohesperidin suppress TGF- β 1-induced Smad3 activation/phosphorylation? One possible explanation is that neohesperidin blocks the interaction between TGF- β 1 receptor and Smad3. Further, why is neohesperidin less effective in the inflammatory stage of bleomycin model of fibrosis and will it have the same effect on other models, such as silica-induced pulmonary fibrosis? In addition, our findings would have been more significant had we used primary human cells instead of A549 (human alveolar type-II epithelial cell line) and MLg (mouse lung fibroblast cell line) cells for *in vitro* experiments.

In summary, our study indicated that neohesperidin attenuated bleomycin-induced pulmonary fibrosis and dysfunction in mice. We postulated that the mechanism of action of neohesperidin involved in the protection against epithelial injury, inhibition of myofibroblast differentiation, ECM deposition, and fibroblast migration is via negative regulation of TGF- β 1/Smad3 signaling pathway. The use of neohesperidin as a potential therapeutic

strategy for patients with progressive pulmonary fibrosis is promising because of its low toxicity and the ability to reverse pulmonary fibrosis without affecting the inflammatory response to different lung injuries.

Acknowledgement

This work was supported by the Tianjin Research Program of Application Foundation and Advanced Technology (15JCYBJC29100), National Natural Science Foundation of China (grants 81430001 and 31471373), State Key Laboratory of Medicinal Chemical Biology, Nankai University (201602004), and State Key Laboratory of Natural Medicines, China Pharmaceutical University (SKLNMKF201409).

Conflicts of interest

The authors declare no conflict of interest.

References

- Agostini, C., Gurrieri, C., 2006. Chemokine/cytokine cocktail in idiopathic pulmonary fibrosis. *Proc Am Thorac Soc.* 3, 357-363.
- Bellocco, E., Barreca, D., Lagana, G., Leuzzi, U., Tellone, E., Ficarra, S., Kotyk, A., Galtieri, A., 2009. Influence of l-rhamnosyl-d-glucosyl derivatives on properties and biological interaction of flavonoids. *Mol Cell Biochem.* 321, 165-171.
- Byrne, A.J., Maher, T.M., Lloyd, C.M., 2016. Pulmonary Macrophages: A New Therapeutic Pathway in Fibrosing Lung Disease? *Trends in Molecular Medicine.* 22, 303-316.

Dong, Y.Y., Geng, Y., Li, L., Li, X.H., Yan, X.H., Fang, Y.S., Li, X.X., Dong, S.Y., Liu, X., Li, X., Yang, X.H., Zheng, X.H., Xie, T., Liang, J.R., Dai, H.P., Liu, X.Q., Yin, Z.N., Noble, P.W., Jiang, D.H., Ning, W., 2015. Blocking follistatin-like 1 attenuates bleomycin-induced pulmonary fibrosis in mice. *J Exp Med.* 212, 235-252.

Duncan, M.R., Frazier, K.S., Abramson, S., Williams, S., Klapper, H., Huang, X.F., Grotendorst, G.R., 1999. Connective tissue growth factor mediates transforming growth factor beta-induced collagen synthesis: downregulation by cAMP. *Faseb J.* 13, 1774-1786.

Fang, Y., Zhang, S., Li, X., Jiang, F., Ye, Q., Ning, W., 2017. Follistatin like-1 aggravates silica-induced mouse lung injury. *Sci Rep.* 7, 399.

Guan, R., Wang, X., Zhao, X., Song, N., Zhu, J., Wang, J., Wang, J., Xia, C., Chen, Y., Zhu, D., Shen, L., 2016. Emodin ameliorates bleomycin-induced pulmonary fibrosis in rats by suppressing epithelial-mesenchymal transition and fibroblast activation. *Sci Rep.* 6, 35696.

Hinz, B., Phan, S.H., Thannickal, V.J., Prunotto, M., Desmouliere, A., Varga, J., De Wever, O., Mareel, M., Gabbian, G., 2012. Recent Developments in Myofibroblast Biology Paradigms for Connective Tissue Remodeling. *Am J Pathol.* 180, 1340-1355.

Hoyles, R.K., Derrett-Smith, E.C., Khan, K., Xu, S.W., Howat, S.L., Wells, A.U., Abraham, D.J., Denton, C.P., 2011. An Essential Role for Resident Fibroblasts in Experimental Lung Fibrosis Is Defined by Lineage-Specific Deletion of High-Affinity Type II Transforming Growth Factor beta Receptor. *Am J Resp Crit Care.* 183, 249-261.

Hoyt, D.G., Lazo, J.S., 1988. Alterations in pulmonary mRNA encoding procollagens,

fibronectin and transforming growth factor-beta precede bleomycin-induced pulmonary fibrosis in mice. *J Pharmacol Exp Ther.* 246, 765-771.

Hu, H.H., Chen, D.Q., Wang, Y.N., Feng, Y.L., Cao, G., Vaziri, N.D., Zhao, Y.Y., 2018. New insights into TGF-beta/Smad signaling in tissue fibrosis. *Chem-Biol Interact.* 292, 76-83.

Huang, X., He, Y., Chen, Y., Wu, P., Gui, D., Cai, H., Chen, A., Chen, M., Dai, C., Yao, D., Wang, L., 2016. Baicalin attenuates bleomycin-induced pulmonary fibrosis via adenosine A2a receptor related TGF-beta1-induced ERK1/2 signaling pathway. *Bmc Pulm Med.* 16, 132.

Hwang, S.L., Yen, G.C., 2008. Neuroprotective effects of the citrus flavanones against H₂O₂-induced cytotoxicity in PC12 cells. *J Agr Food Chem.* 56, 859-864.

Jia, S., Hu, Y., Zhang, W.N., Zhao, X.Y., Chen, Y.H., Sun, C.D., Li, X., Chen, K.S., 2015. Hypoglycemic and hypolipidemic effects of neohesperidin derived from *Citrus aurantium* L. in diabetic KK-A(y) mice. *Food Funct.* 6, 878-886.

Jiang, D.H., Liang, J.R., Hodge, J., Lu, B., Zhu, Z., Yu, S., Fan, J., Gao, Y.F., Yin, Z.N., Homer, R., Gerard, C., Noble, P.W., 2004. Regulation of pulmonary fibrosis by chemokine receptor CXCR3. *J Clin Invest.* 114, 291-299.

Kang, J.H., Jung, M.Y., Yin, X., Andrianifahanana, M., Hernandez, D.M., Leof, E.B., 2017. Cell-penetrating peptides selectively targeting SMAD3 inhibit profibrotic TGF-beta signaling. *J Clin Invest.* 127, 2541-2554.

Khalil, N., O'Connor, R.N., Unruh, H.W., Warren, P.W., Flanders, K.C., Kemp, A., Berezney, O.H., Greenberg, A.H., 1991. Increased production and immunohistochemical localization of transforming growth factor-beta in idiopathic pulmonary fibrosis. *Am J Resp Cell Mol.* 5, 155-162.

King, T.E., Jr., Pardo, A., Selman, M., 2011. Idiopathic pulmonary fibrosis. *Lancet.* 378, 1949-1961.

Lee, J.H., Lee, S.H., Kim, Y.S., Jeong, C.S., 2009. Protective Effects of Neohesperidin and Poncirin Isolated from the Fruits of *Poncirus trifoliata* on Potential Gastric Disease. *Phytother Res.* 23, 1748-1753.

Li, M., Krishnaveni, M.S., Li, C.G., Zhou, B.Y., Xing, Y.M., Banfalvi, A., Li, A.M., Lombardi, V., Akbari, O., Borok, Z., Minoo, P., 2011. Epithelium-specific deletion of TGF-beta receptor type II protects mice from bleomycin-induced pulmonary fibrosis. *J Clin Invest.* 121, 277-287.

Liu, B., Cao, B., Zhang, D., Xiao, N., Chen, H., Li, G.Q., Peng, S.C., Wei, L.Q., 2016. Salvianolic acid B protects against paraquat-induced pulmonary injury by mediating Nrf2/Nox4 redox balance and TGF-beta 1/Smad3 signaling. *Toxicol Appl Pharm.* 309, 111-120.

Meng, X.M., Huang, X.R., Chung, A.C.K., Qin, W., Shao, X.L., Igarashi, P., Ju, W.J., Bottinger, E.P., Lan, H.Y., 2010. Smad2 Protects against TGF-beta/Smad3-Mediated Renal Fibrosis. *Journal of the American Society of Nephrology.* 21, 1477-1487.

- Moeller, A., Ask, K., Warburton, D., Gauldie, J., Kolb, M., 2008. The bleomycin animal model: A useful tool to investigate treatment options for idiopathic pulmonary fibrosis? *Int J Biochem Cell B.* 40, 362-382.
- Mora, A.L., Rojas, M., Pardo, A., Selman, M., 2017. Emerging therapies for idiopathic pulmonary fibrosis, a progressive age-related disease. *Nat Rev Drug Discov.* 16, 755-772.
- Ning, W., Li, C.J., Kaminski, N., Feghali-Bostwick, C.A., Alber, S.M., Di, Y.P., Otterbein, S.L., Song, R., Hayashi, S., Zhou, Z., Pinsky, D.J., Watkins, S.C., Pilewski, J.M., Sciruba, F.C., Peters, D.G., Hogg, J.C., Choi, A.M., 2004. Comprehensive gene expression profiles reveal pathways related to the pathogenesis of chronic obstructive pulmonary disease. *Proc Natl Acad Sci U S A.* 101, 14895-14900.
- Noble, P.W., Barkauskas, C.E., Jiang, D., 2012. Pulmonary fibrosis: patterns and perpetrators. *J Clin Invest.* 122, 2756-2762.
- Raghu, G., Brown, K.K., Bradford, W.Z., Starko, K., Noble, P.W., Schwartz, D.A., King, T.E., Adlakha, A., Tarczynski, S., Ainslie, G., Kalam, R., Bai, T., Truchan, H., Baughman, R., Wingst, D., Bhorade, S., Norwick, L., Brown, K.K., Kervitsky, D., Calhoun, W., DiNella, L., Chan, C., Jamieson, L., Chan, K., Turpen, T., Chapman, J., Slattery, S., Chen, L., Turner, J., Clark, M., Sanders, R., Crain, M., Pate, D., Davis, G., Lynn, M., Dhar, A., Hrytsyk, M., Drent, M., Horr, E.T., du Bois, R., Goh, N., Egan, J., Anthony, N., Enelow, R., Haram, T., Ettinger, N., Merli, S., Frost, A., Holy, R., Glassberg, M., Brown, A., Golden, J., DesMarais, M., Haim, Y.D., Rzeszutko, B., Hassoun, P., Finlay, G., Lawler, L., Hollingsworth, H., Goncalves, P., Jackson, R., Meadows, T., Kallay, M., Celebie, A., King-Biggs, M., Beyle, A.,

Lancaster, L., Sanderson, R., Lasky, J., Ditta, S., Lorch, D., Schoh, T., Lynch, J., Alousha, A., Mageto, Y., Meachom, M., Martinez, F., Dahlgren, D., McKee, C., Hamilton, T., Meyer, K., Wilson, S., Millar, A., Hann, A., Mohsenifar, Z., Balfe, D., Morell, F., Reyes, L., Nathan, S., Theodoslod, S., Noble, P.W., Shrauger, K., Noth, I., Streck, M., Au, J., Olivier, K., Wells, R., Padilla, M., Behnegar, A., Polito, A., Bloom, C., Raghu, G., Snydsman, A., Rosen, G., Jacobs, S., Ryu, J.H., Carlson, K., Sahn, S.A., Oser, R., Schaumberg, T., Chesnutt, M., Leonard, S., Schluger, N., Jellen, P., Steele, M., Willis, C., Strieter, R., Christedoulou, V., Valentine, V., Lanning, T., Wencel, M., Sturgeon, D., Xaubert, A., Zisman, D., Douglas, L., Lynch, D.A., Godwin, J.D., Webb, W.R., Fleming, T., Reis, A., Riley, D., Stud, I.P.F., 2004. A placebo-controlled trial of interferon gamma-1b in patients with idiopathic pulmonary fibrosis. *New England Journal of Medicine*. 350, 125-133.

Raghu, G., Weycker, D., Edelsberg, J., Bradford, W.Z., Oster, G., 2006. Incidence and prevalence of idiopathic pulmonary fibrosis. *Am J Respir Crit Care Med*. 174, 810-816.

Selman, M., Pardo, A., 2012. Alveolar epithelial cell disintegrity and subsequent activation: a key process in pulmonary fibrosis. *Am J Respir Crit Care Med*. 186, 119-121.

Sime, P.J., Xing, Z., Graham, F.L., Csaky, K.G., Gauldie, J., 1997. Adenovector-mediated gene transfer of active transforming growth factor-beta1 induces prolonged severe fibrosis in rat lung. *J Clin Invest*. 100, 768-776.

Suganuma, H., Sato, A., Tamura, R., Chida, K., 1995. Enhanced migration of fibroblasts derived from lungs with fibrotic lesions. *Thorax*. 50, 984-989.

Wang, X.-t., Sun, X.-j., Li, C., Liu, Y., Zhang, L., Li, Y.-d., Wu, Q.-h., Li, S.-y., Li, Y., 2018.

Establishing a Cell-Based High-Content Screening Assay for TCM Compounds with Anti-Renal Fibrosis Effects. *Evidence-Based Complementary and Alternative Medicine*. 2018, 1-10.

Wolters, P.J., Collard, H.R., Jones, K.D., 2014. Pathogenesis of idiopathic pulmonary fibrosis. *Annu Rev Pathol*. 9, 157-179.

Wynn, T.A., 2011. Integrating mechanisms of pulmonary fibrosis. *J Exp Med*. 208, 1339-1350.

Xu, F., Zang, J., Chen, D., Zhang, T., Zhan, H., Lu, M., Zhuge, H., 2012. Neohesperidin induces cellular apoptosis in human breast adenocarcinoma MDA-MB-231 cells via activating the Bcl-2/Bax-mediated signaling pathway. *Nat Prod Commun*. 7, 1475-1478.

Yagi, K., Goto, D., Hamamoto, T., Takenoshita, S., Kato, M., Miyazono, K., 1999.

Alternatively spliced variant of Smad2 lacking exon 3 - Comparison with wild-type Smad2 and Smad3. *J Biol Chem*. 274, 703-709.

Figure legends

Fig. 1. Neohesperidin (NHP) suppresses TGF- β 1-activated Smad3 signaling *in vitro*.

(A) Chemical structure of neohesperidin. (B) CAGA-NIH-3T3 reporter cells were pretreated with neohesperidin at different concentrations for 1 h and then cultured with or without TGF- β 1 (5 ng/ml) for 24 h, followed by lysis for the luciferase assay (n = 3). * P < 0.05, ** P < 0.01 versus [0 μ M neohesperidin + TGF- β 1] group. ANOVA followed by Tukey's test. (C) MLg cells were treated with neohesperidin (20 μ M) for 1 h before TGF- β 1 (5 ng/ml) treatment for 30 min. The levels of phosphorylation of Smad3, Smad2, ERK, p38, and JNK were determined by western blotting. GAPDH was used as a loading control. For each protein, the ratio of its phosphorylated fraction to the total protein level was calculated based on the densities of the respective bands (n = 3). ** P < 0.01. ANOVA followed by Tukey's test.

Fig. 2. Neohesperidin (NHP) inhibits TGF- β 1-induced fibroblast activation, ECM production, and fibroblast migration *in vitro*.

(A) MLg cells were treated with or without TGF- β 1 (5 ng/ml) in the absence or presence of neohesperidin for 48 h. Effects of neohesperidin (0–200 μ M) on cell viability were determined using the MTT assay (n = 5). ** P < 0.01 versus [0 μ M neohesperidin + TGF- β 1] group; α , P < 0.01 versus [0 μ M neohesperidin – TGF- β 1] group. ANOVA followed by Tukey's test. (B–D) qRT-PCR analysis of *Acta2* (B), *Coll1a1* (C), and *Fnl* (D) mRNA expression (n = 3). ** P < 0.05, ** P < 0.01 versus [0 μ M neohesperidin + TGF- β 1]. ANOVA followed by Tukey's test. (E) Western blot analysis of α -SMA in cell extracts (Cell) and Coll1

and Fn1 in the medium supernatant (SN). β -tubulin was used as a loading control. Expression levels of α -SMA were normalized to those of β -tubulin based on the densities of the respective bands ($n = 3$). (F) A wound healing assay was used to assess the effect of neohesperidin on fibroblast migration. The wound closure was photographed 36 h post-scratching. Original magnification, $\times 40$. (G) The wound closure rate, representing the migration rate, was determined at 36 h ($n = 3$). (E and G) $*P < 0.05$, $**P < 0.01$ versus [0 μ M neohesperidin + TGF- β 1] group; α , $P < 0.01$ versus [0 μ M neohesperidin – TGF- β 1] group. ANOVA followed by Tukey's test.

Fig. 3. Neohesperidin (NHP) suppresses TGF- β 1-induced epithelial injury *in vitro*.

A549 cells were treated with TGF- β 1 (10 ng/ml) and different concentrations of neohesperidin for 24 or 48 h. (A and B) Epithelial injury was determined by examining the expression levels of E-cadherin, N-cadherin, and SNAIL. β -tubulin was used as a loading control. Expression levels of E-cadherin, N-cadherin, and SNAIL were normalized to those of β -tubulin based on the densities of the respective bands ($n = 3$). $*P < 0.05$, $**P < 0.01$. ANOVA followed by Tukey's test. (C–E) A549 cells were treated with TGF- β 1 (10 ng/ml) and different concentrations of neohesperidin for 24 h, and relative expression of *CDH1*, *CDH2*, and *SNAIL* were determined by qRT-PCR ($n = 3$). $*P < 0.05$, $**P < 0.01$. ANOVA followed by Tukey's test (C and E) and Kruskal–Wallis followed by Dunn's test (B).

Fig. 4. Neohesperidin (NHP) increases the survival rate and improves pulmonary function of bleomycin (BLM)-injured mice.

(A) Schematic representation of the timeline of therapeutic dosing of neohesperidin (20 mg/kg) or CMC-Na (vehicle control) to mice with established fibrosis following bleomycin-induced lung injury. (B) Percentages of survived mice were plotted over a 21-day period after bleomycin treatment. A log-rank test was used to compare the difference between the CMC-Na and neohesperidin treatment groups ($n = 21$ and $n = 17$, respectively); $P = 0.0378$. (C–E) Pulmonary function parameters, including respiratory dynamic compliance (C_{dyn}), resistance of the lung (RL), and resistance of expiration (RE), were calculated for different groups (Saline group: $n = 6$; BLM + CMC-Na group: $n = 4$; BLM + NHP group: $n = 7$). Mice injected intratracheally with saline were used as a sham control. $*P < 0.05$, $**P < 0.01$. Kruskal–Wallis followed by Dunn’s test (C) and ANOVA followed by Tukey’s test (D and E).

Fig. 5. Neohesperidin (NHP) attenuates bleomycin (BLM)-induced lung fibrosis in mice.

(A) Interventional dosing regimen in an early-stage lung fibrosis model. C57BL/6J mice were i.p. injected with CMC-Na (vehicle control) or neohesperidin (20 mg/kg) at the indicated times after bleomycin treatment, and lungs were harvested on day 14. Mice injected intratracheally with saline were used as a sham control (Saline group: $n = 5$; BLM + CMC-Na group: $n = 6$; BLM + NHP group: $n = 7$). (B) Body weight at 14 days was compared with that at baseline. (C) Hydroxyproline contents in lung tissues. (D) Representative images of lung sections stained with hematoxylin and eosin (H&E) and Masson’s trichrome. Bar = 100 μm . (E) Lung fibrotic score analysis shows percentages of fibrotic areas in lung sections. Mice intratracheally injected with saline were used as a sham control. (B, C and E) $*P < 0.05$,

**** $P < 0.01$.** ANOVA followed by Tukey's test. (F) Western blotting of Col1 and α -SMA in lung tissues. GAPDH was used as a loading control. Expression levels of the target proteins were normalized to those of GAPDH based on the densities of the respective bands. (G) Levels of phosphorylation of Smad3 and Smad2 in lung tissues were determined by western blotting. β -actin was used as a loading control. The ratios of p-Smad3 and p-Smad2 to their total levels were calculated based on the densities of the respective bands ($n = 3$ per group). (F and G) *** $P < 0.05$, ** $P < 0.01$.** ANOVA followed by Tukey's test.

Fig. 6. Neohesperidin (NHP) attenuates existing lung fibrosis in bleomycin (BLM)-injured mice.

(A) Interventional dosing regimen in a late-stage lung fibrosis model. C57BL/6J mice were i.p. injected with CMC-Na (vehicle control) or neohesperidin (20 mg/kg) at the indicated times after bleomycin treatment, and lungs were harvested on day 21. Mice injected intratracheally with saline were used as a sham control (Saline group: $n = 4$; BLM + CMC-Na group: $n = 7$; BLM + NHP group: $n = 7$). (B) Body weight at 21 days was compared with that at baseline. (C) Hydroxyproline contents in lung tissues. (D) Representative images of lung sections stained with hematoxylin and eosin (H&E) and Masson's trichrome. Bar = 100 μm . (E) Lung fibrotic score analysis shows percentages of fibrotic areas in lung sections. (B, C and E) *** $P < 0.05$, ** $P < 0.01$.** ANOVA followed by Tukey's test.

Fig. 7. Neohesperidin (NHP) does not affect the inflammatory response after bleomycin

treatment.

(A) C57BL/6J mice were i.p. injected with CMC-Na (vehicle control) or neohesperidin (20 mg/kg) daily from day 1 after bleomycin challenge until day 6 and killed on day 7 for analysis of inflammation ($n = 4$ per group). (B) Total numbers of BALF cells were determined using a hemocytometer. (C) Differential cell counts in BALF [macrophages, lymphocytes, and polymorphonuclear neutrophils (PMNs)] were determined according to the standard morphological criteria. (D–F) Levels of IL-1 β (D), IFN- γ (E), and TNF- α (F) in BALF were determined by ELISAs.

Fig. 8. Neohesperidin (NHP) does not prevent fibrosis in mice.

(A) Time course of neohesperidin administration, bleomycin challenge, and fibrosis testing in a prophylactic model. (B) Hydroxyproline contents in lung tissues. (C) Representative images of lung sections stained with Masson's trichrome. Bar = 100 μ m. (D) Lung fibrotic score analysis shows percentages of fibrotic areas in lung sections.

Figure 1

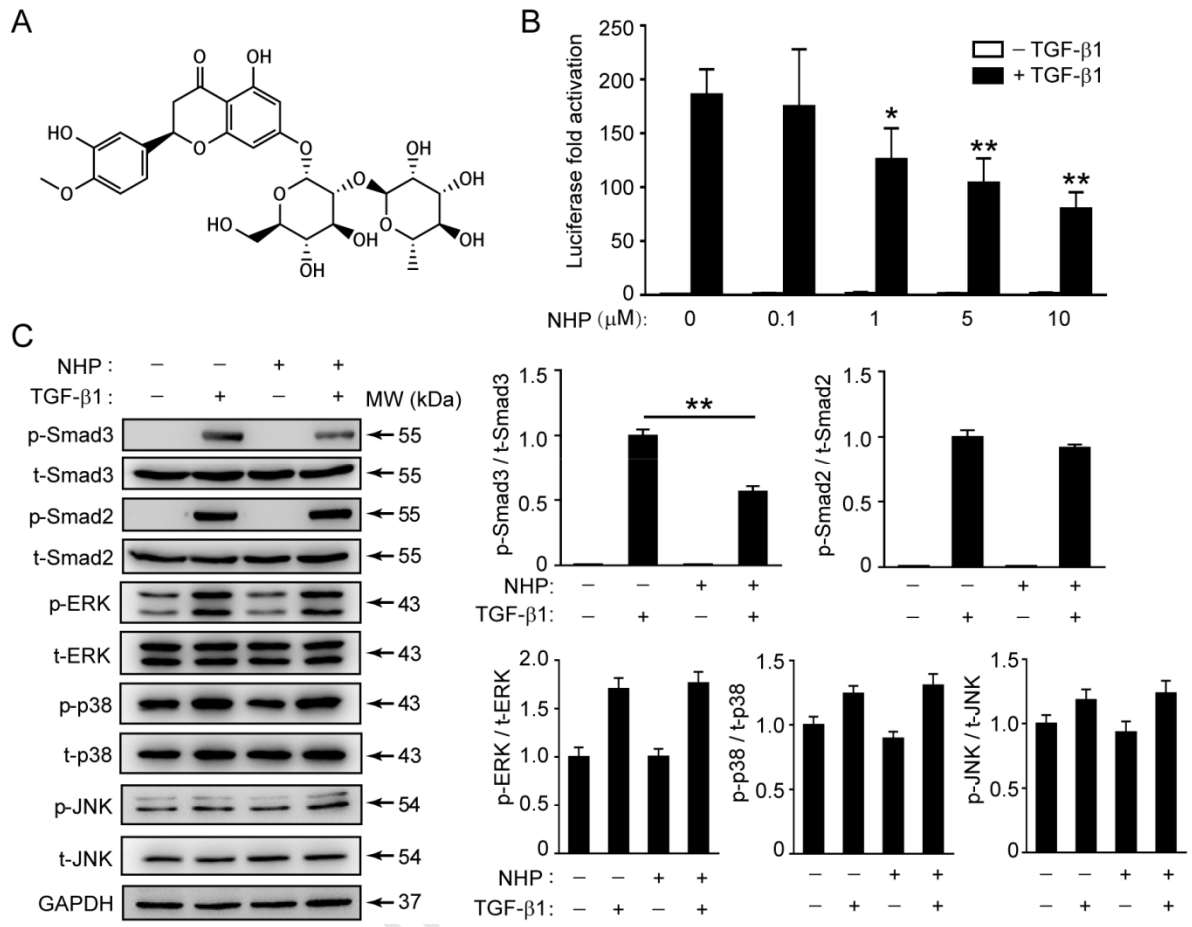


Figure 2

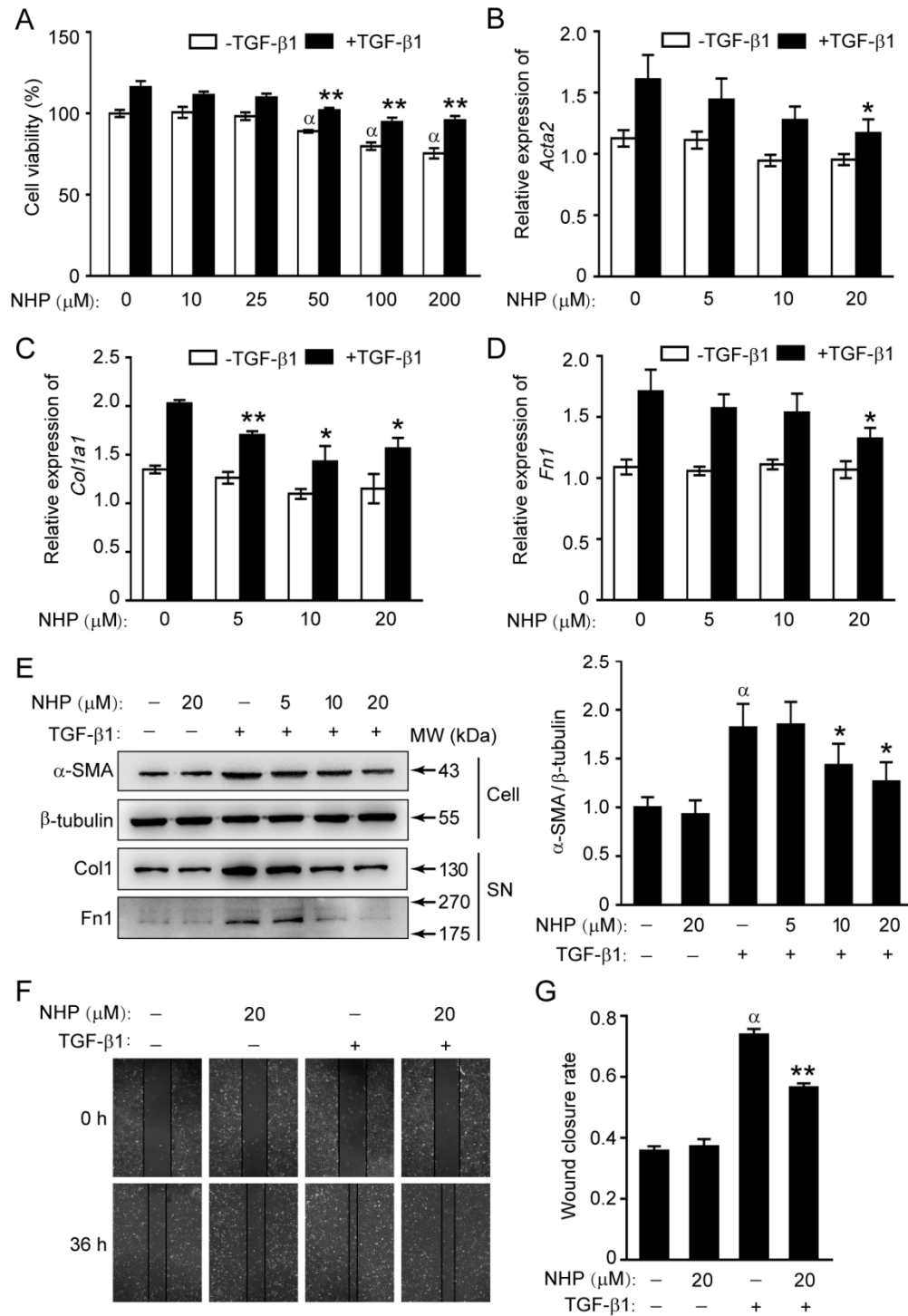


Figure 3

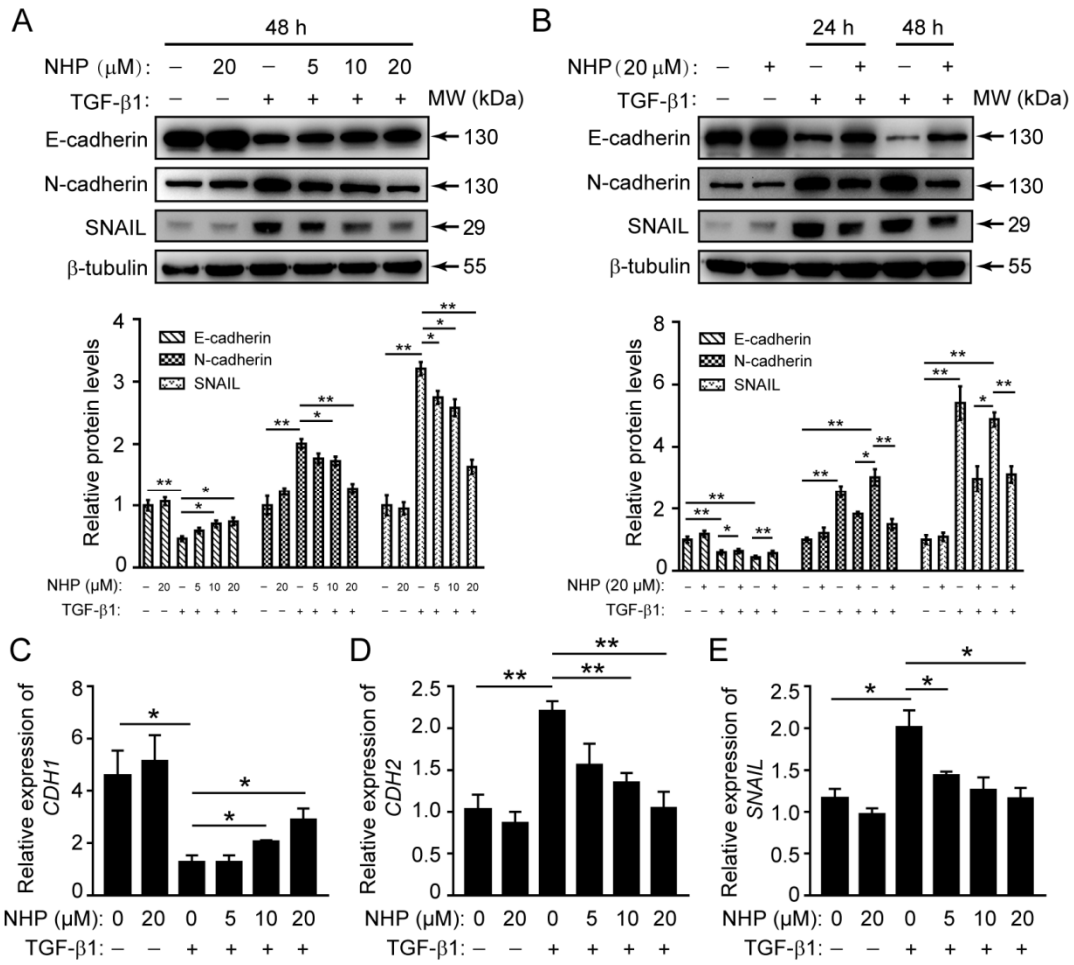


Figure 4

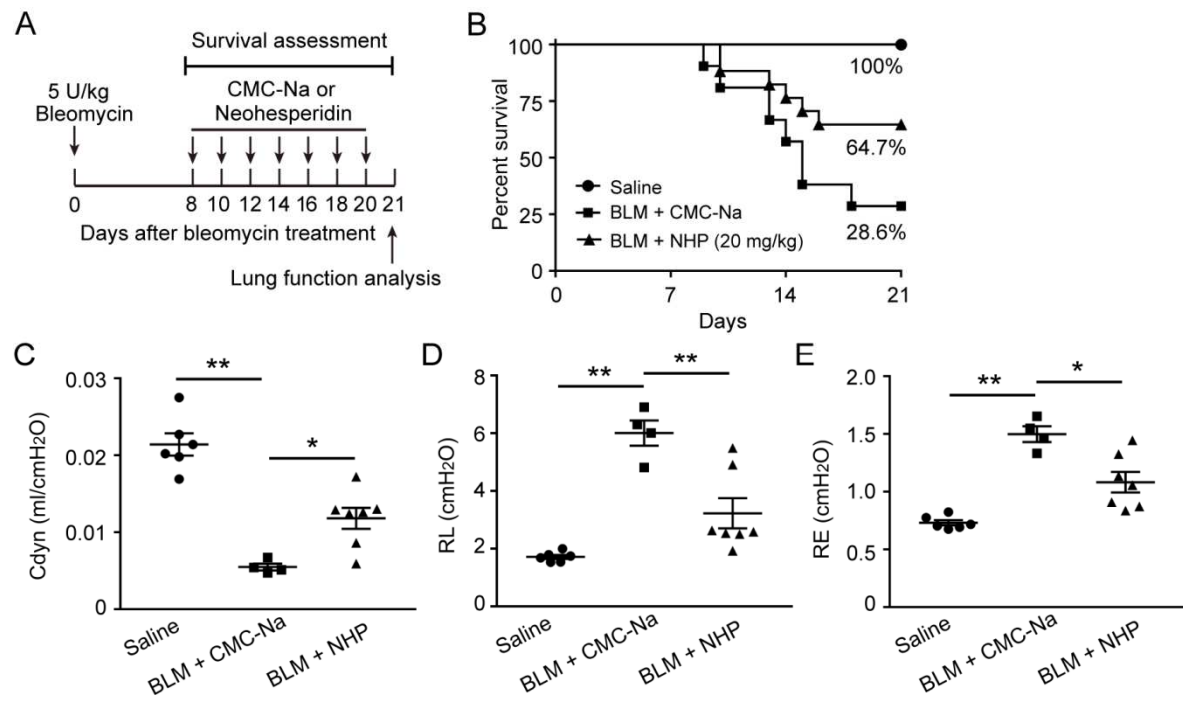


Figure 5

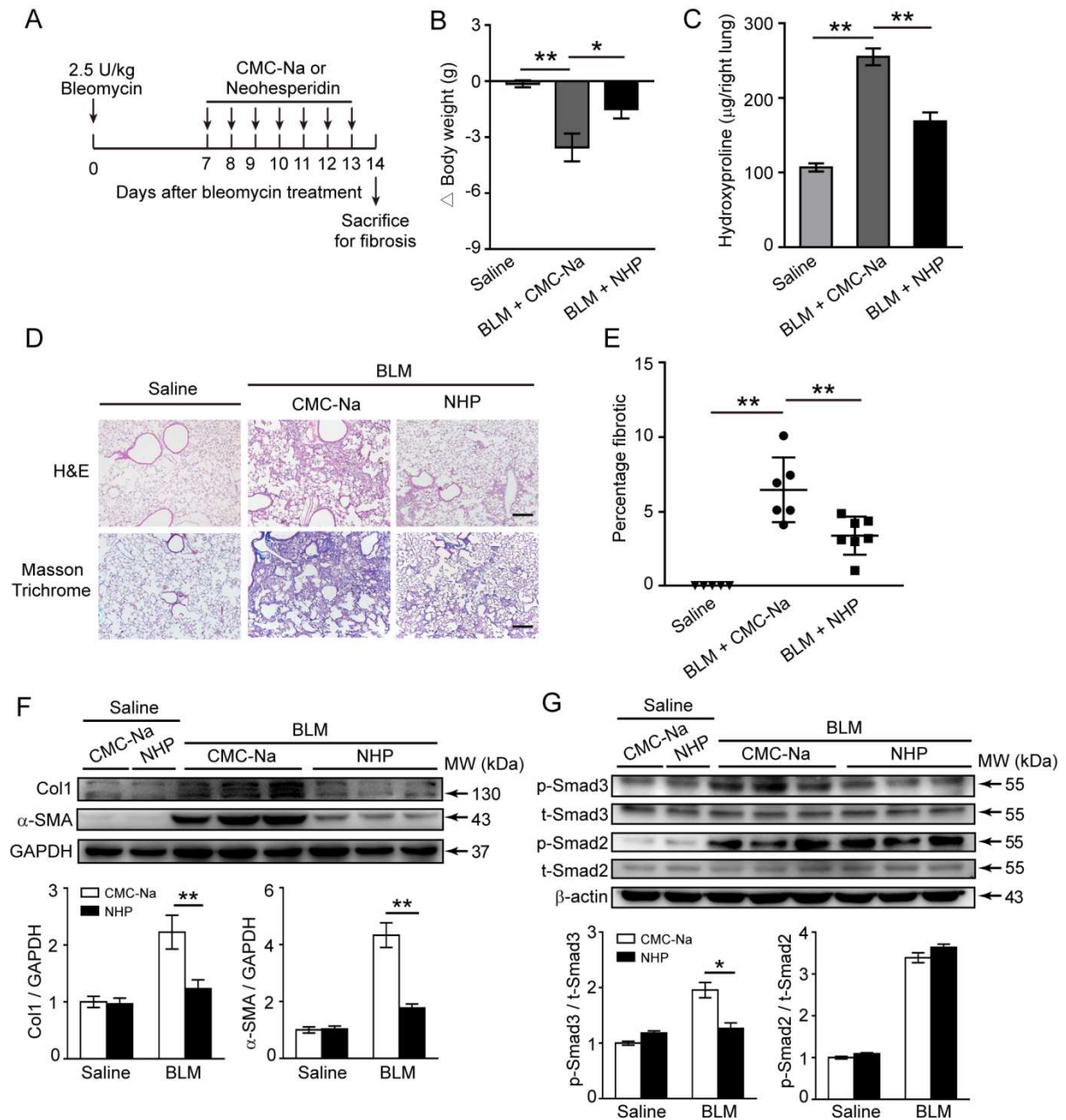


Figure 6

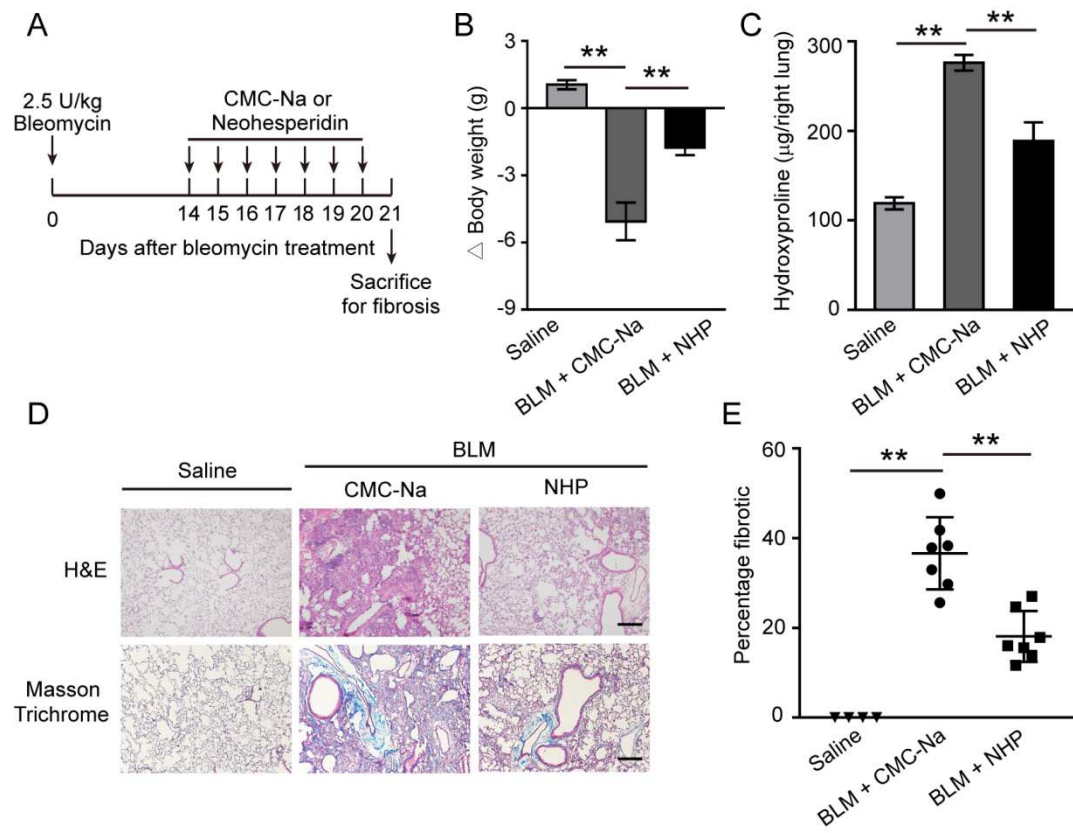


Figure 7

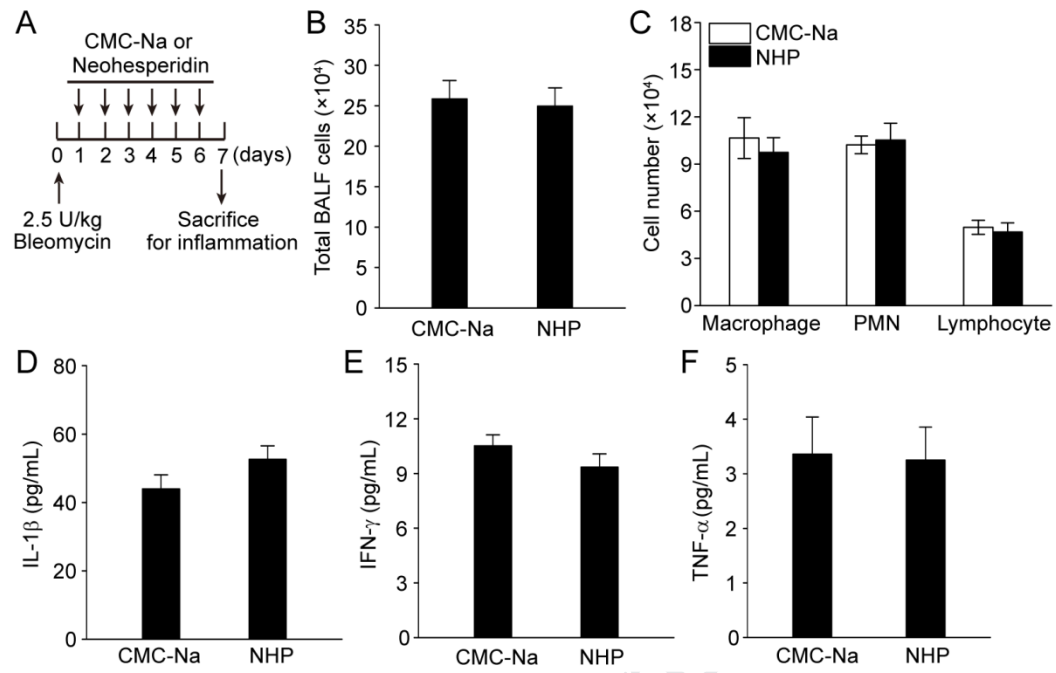
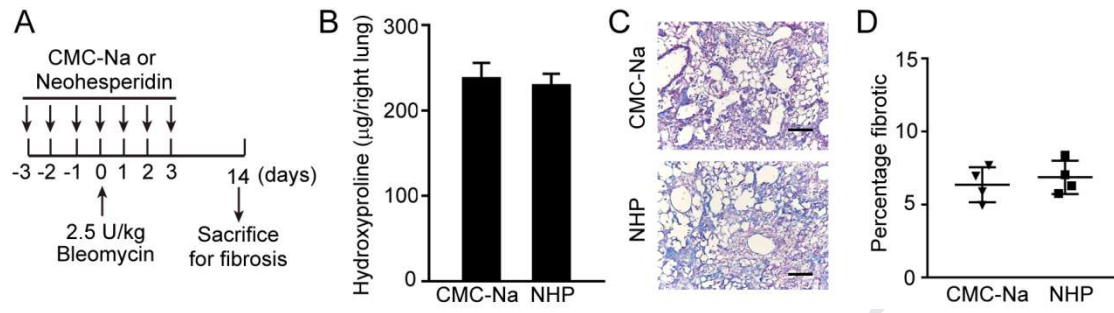


Figure 8



CRedit Author Statement

Jiasen Guo: Investigation, Methodology, Writing-Original draft preparation, Writing-Reviewing and Editing. **Yinshan Fang:** Data curation, Validation, Writing-Original draft preparation, Software. **Fangxin Jiang:** Data curation, Investigation. **Lian Li:** Supervision. **Honggang Zhou:** Formal Analysis, Validation. **Xiaojun Xu:** Supervision, Resources, Conceptualization. **Wen Ning:** Conceptualization, Writing-Reviewing and Editing, Project Administration, Funding Acquisition.